AIP | Review of Scientific Instruments

Real-time inverse hysteresis compensation of piezoelectric actuators with a modified Prandtl-Ishlinskii model

Guo-Ying Gu, Mei-Ju Yang, and Li-Min Zhu

Citation: Rev. Sci. Instrum. **83**, 065106 (2012); doi: 10.1063/1.4728575
View online: http://dx.doi.org/10.1063/1.4728575
View Table of Contents: http://rsi.aip.org/resource/1/RSINAK/v83/i6
Published by the American Institute of Physics.

Real-time inverse hysteresis compensation of piezoelectric actuators with a modified Prandtl-Ishlinskii model

Guo-Ying Gu, Mei-Ju Yang, and Li-Min Zhu[a]
State Key Laboratory of Mechanical System and Vibration, School of Mechanical Engineering, Shanghai Jiao Tong University, Shanghai 200240, China

(Received 11 December 2011; accepted 28 May 2012; published online 11 June 2012)

This paper presents a novel real-time inverse hysteresis compensation method for piezoelectric actuators exhibiting asymmetric hysteresis effect. The proposed method directly utilizes a modified Prandtl-Ishlinskii hysteresis model to characterize the inverse hysteresis effect of piezoelectric actuators. The hysteresis model is then cascaded in the feedforward path for hysteresis cancellation. It avoids the complex and difficult mathematical procedure for constructing an inversion of the hysteresis model. For the purpose of validation, an experimental platform is established. To identify the model parameters, an adaptive particle swarm optimization algorithm is adopted. Based on the identified model parameters, a real-time feedforward controller is implemented for fast hysteresis compensation. Finally, tests are conducted with various kinds of trajectories. The experimental results show that the tracking errors caused by the hysteresis effect are reduced by about 90%, which clearly demonstrates the effectiveness of the proposed inverse compensation method with the modified Prandtl-Ishlinskii model.
[http://dx.doi.org/10.1063/1.4728575]

I. INTRODUCTION

With the increasing development of nanoscience and nanotechnology, piezoelectric actuators with nanometer or sub-nanometer positioning resolution have been widely applied for actuation in various industrial applications such as scanning probe microscopes (SPMs),[1] atomic force microscopes (AFMs),[2,3] and micromanipulation.[4,5] However, a major disadvantage of piezoelectric actuators is the complex voltage-displacement hysteresis nonlinearity as depicted in Fig. 1. Owing to its non-smooth and non-memoryless nature as well as multi-valuedness, hysteresis usually causes severe limitations on the performances (tracking precision and stability, etc.) of piezoelectric actuators.[6,7] Alternatively, hysteresis can be significantly reduced if piezoelectric actuators are driven by a charge amplifier rather than a voltage amplifier.[8,9] However, the charge amplifier has not been widely adopted due to its implementation complexity and cost.[9,10] To date, the voltage amplifier is still the most popular approach to drive piezoelectric actuators. In this case, development of control techniques to mitigate the effect of hysteresis in piezoelectric actuators has attracted significant attentions.

Feedback control techniques seem to be the best way to reach overall substantial performances in terms of accuracy, disturbances, vibration, and uncertainty rejection.[11] However, feedback control techniques strongly depend on the integration of the bulky sensors, which generally leads to the difficulty for fabrication in such small systems like piezo-actuated nanopositioning stages or micromanipulation.[12] Another challenge for feedback control of piezoelectric actuators lies on the fact that they are nonlinear systems with non-smooth nonlinearities for which traditional control methods are insufficient.[13] A feedforward control technique is an alternative way to remedy the hysteresis,[3,12,14] which is desired to employ an inverse of the hysteresis for compensation. As a result, the series connection of the inverse and the real actuator can be approximated as a quasi-linear system for which simple and traditional control strategies are available.[15] For this purpose, many works have been accomplished. Using the Preisach model, Ge and Jouaneh[16] applied a numerical inverse Preisach model as a feedforward compensator to linearize the hysteresis nonlinearity, and extensive works have then been developed in Refs. 17–19. Considering that the Preisach model is not analytically invertible, numerical methods are generally adopted to obtain approximate inversions of the model. As a subclass of the Preisach model, the Prandtl-Ishlinskii (P-I) model is another effective method to describe the hysteresis nonlinearity by a single threshold variable.[20] The main advantages of the P-I model over the Preisach model are the reduced modeling complexity and the analytical inverse for the P-I model, thus making it more efficient for real-time applications. Krejci[21] first presented an analytical inverse expression for the classical P-I model to cancel the symmetric hysteresis nonlinearity. For asymmetric hysteresis cancellation, Kuhnen[22] developed a modified P-I model by introducing the deadzone operators to generate an inverse feedforward controller. Using two different envelope functions based play operators, a generalized P-I model[23] is proposed to compensate for the asymmetric and saturated hysteresis effect. In addition, other hysteresis models[24–28] with specific characteristics have also been proposed to develop feedforward controllers for inverse hysteresis compensation.

In the above literature, on inverse hysteresis compensation, the design procedures generally consist of modeling the real hysteresis nonlinearity, identifying the model parameters

[a]Electronic mail: zhulm@sjtu.edu.cn.

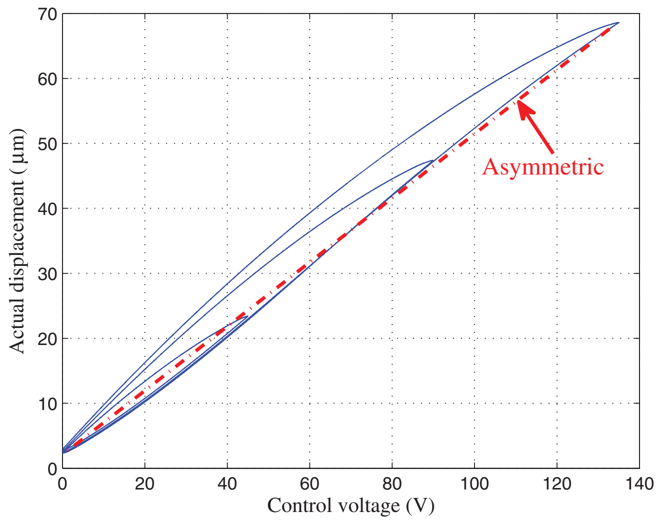

FIG. 1. Hysteresis curves of a piezoelectric actuator.

to match the real hysteresis and constructing an inverse model as a desired compensator. The mathematical complexity of the identification and inversion problem depends on the selected modeling approaches. Different from the commonly used procedures, a direct inverse hysteresis compensation method is proposed in this work. The new concept is motivated by the fact that the inversion of the hysteresis effect is by nature hysteresis loops. The difference between the inverse hysteresis and the real hysteresis in piezoelectric actuator is the orientation of the hysteresis loops. From the mathematical point of view, an available hysteresis model can be directly applied to characterize the inverse hysteresis effect instead of modeling the real hysteresis nonlinearity. Subsequently, the identified hysteresis model can be directly cascaded in the feedforward path for hysteresis cancellation, which thus avoids the complex and difficult mathematical procedure for developing an inversion of the identified hysteresis model.

As far as we know, only one reported work employed the similar idea of directly modeling the inverse hysteresis effect, which was accomplished by Professor Devasia's group at University of Washington.[29] However, it is quite difficult to develop a real-time feedforward controller because of the great computational cost for calculation with the Preisach model. In fact, the real-time hysteresis compensation requires the availability of sufficiently fast algorithms for implementation. In addition, the experimental verification with different motion trajectories was not addressed in their work. As a subclass of the Preisach model, the P-I model is more efficient for real-time applications.[21] However, the classical P-I model can only characterize the symmetric hysteresis behavior. To overcome this limitation, a modified P-I model is proposed in this paper to characterize the inverse hysteresis effect of the piezoelectric actuator with the asymmetric behavior, which can be directly utilized for inverse hysteresis compensation. Without using the nonlinear deadzone operators[22] or the nonlinear play operators,[23] the modified P-I model combines weighted one-side play operators and a polynomial input function to describe the inverse hysteresis loops. The hysteresis shapes can be determined by not only the weighted play operators but also the input function. The proposed method along with the improved P-I model in this work is much simpler and easier to be implemented for a real-time controller. To validate the descriptions, an effective informed adaptive particle swarm optimization algorithm[30] is adopted as one of the optimization algorithms to identify the model parameters. Then, the identified modified P-I model is implemented into a real-time feedforward controller for fast inverse hysteresis compensation. Finally, tests are conducted with various kinds of referenced trajectories. The experimental results show that the tracking errors caused by the hysteresis effect are reduced by about 90% with the developed feedforward controller. It therefore demonstrates the effectiveness of the new inverse hysteresis compensation method with the modified P-I model.

II. MODIFIED P-I MODEL

For direct inverse hysteresis compensation, a hysteresis model should be utilized to capture the inverse hysteresis effect. Due to the asymmetric hysteresis characteristic of the piezoelectric actuator as shown in Fig. 1, a modified P-I model is developed in this work on the basis of the classical P-I model. Without using the nonlinear deadzone operators[22] or the nonlinear play operators,[23] the developed modified P-I model combines weighted one-side play operators and a polynomial input function to describe the asymmetric hysteresis effect of the piezoelectric actuator. In the following, the developed model is first introduced.

A. Classical P-I model

The play operator[20] defined with a threshold r is widely applied in the P-I model for hysteresis description. Generally, the one-dimensional play operator can be recognized as a piston with plunger of length $2r$. The output $F_r[x](t)$ is the position of the center of the piston, and the input x is the plunger position. Considering the positive excitation nature of the piezoelectric actuator, an one-side play operator[31] is adopted in this work as follows:

$$\begin{aligned} F_r[x](0) &= f_r(x(0), 0), \\ F_r[x](t) &= f_r(x(t), F_r[x](t_i)) \end{aligned} \tag{1}$$

for $t_i < t \le t_{i+1}$, $0 \le i \le N-1$ with

$$f_r(v, w) = \max(v - r, \min(v, w)), \tag{2}$$

where $0 = t_0 < t_1 < \cdots < t_N = t_E$ is a partition of $[0, t_E]$, such that the function $x(t)$ is monotone on each of the subintervals $[t_i, t_{i+1}]$. The argument of the operator is written in square brackets to indicate the functional dependence, since it maps a function to another function. As an illustration, Fig. 2 shows the transfer characteristics of the one-side play operator.

Remark: It is worth mentioning that the one-side play operator is adopted in this work due to the positive excitation nature of the used piezoelectric actuator. For piezoelectric actuators with a positive and negative excitation, one can easily replace the one-side play operator by the classical play

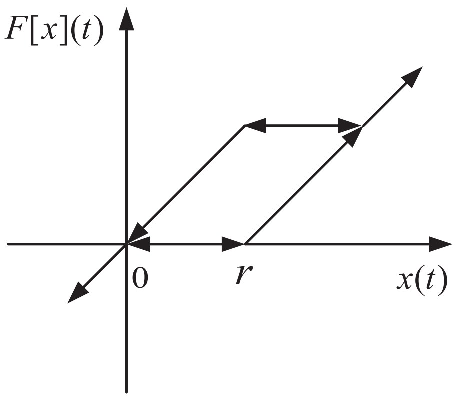

FIG. 2. Input-output relationships of an one-side play operator.

operator. Without losing generality, we use the one-side play operator in this work.

The classical P-I model utilizes the above play operator $F_r[x](t)$ to describe the relationship between output y_p and input x by[20,31]

$$y_p(t) = p_0 x(t) + \int_0^R p(r) F_r[x](t) dr, \tag{3}$$

where $p(r)$ is a density function that is generally calculated from the experimental data, and p_0 is a positive constant. The density function $p(r)$ generally vanishes for large values of r, while the choice of $R = \infty$ as the upper limit of integration is widely used in the literature for the sake of convenience.[21] As discussed in the Introduction, this model has been utilized to characterize and to compensate for the symmetric hysteresis. However, the hysteresis studied in this work exhibits the asymmetric shapes as shown in Fig. 1.

B. Modified P-I model

On the basis of the classical P-I model, a modified P-I model is developed in this work for asymmetric hysteresis description. The developed modified P-I model is defined in terms of the weighed classical play operators and the polynomial input function as follows:

$$y_p(t) = g(x(t)) + \int_0^R p(r) F_r[x](t) dr, \tag{4}$$

where $g(x(t)) = a_1 x^3(t) + a_2 x(t)$ is a polynomial input function with constant a_1 and a_2, $p(r)$ and $F_r[x](t)$ are defined the same as the ones in the classical P-I model (3). It can be seen that the difference between the modified P-I model (4) and the classical P-I model (3) is the selection of the input function $g(x(t))$. The benefit for choosing such an input function is that the modified P-I model can describe the real hysteresis loops in the piezoelectric actuator with asymmetric behaviors. It should be noted that if $g(x(t))$ is selected as $g(x(t)) = p_0 x(t)$, the modified P-I model can be reduced to a classical P-I model. In the following development, it shall be observed that it is the polynomial input function $g(x(t))$ that makes the modified P-I model accommodate a more general class of hysteresis shapes.

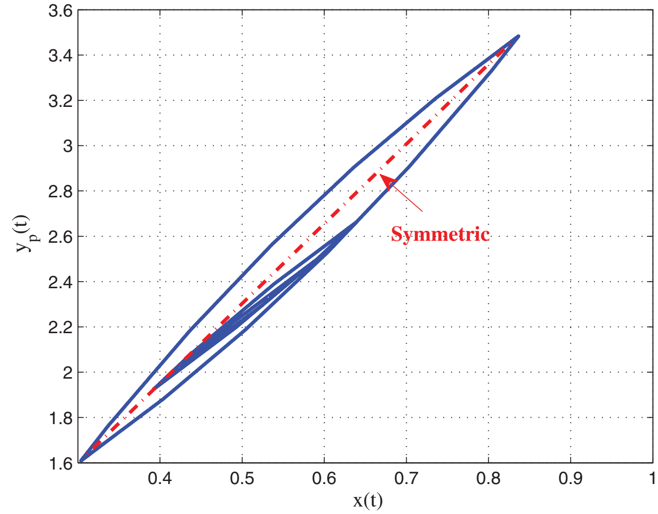

FIG. 3. Hysteresis loops generated by the classical P-I model (3).

As an illustration, Fig. 3 shows the hysteresis loops of the classical P-I model given by $y_p(t) = p_0 x(t) + \int_0^R p(r) F_r[x](t) dr$ with $p_0 = 2.42$, $p(r) = 5e^{-0.505(r-1)^2}$, $r \in [0, 1]$ and the input $x(t) = 0.5 + 0.5\,\sin(3t)/(1+t)$. Using the same density function $p(r)$ and input $x(t)$, the hysteresis loops of the modified P-I model described by $y_p(t) = g(x(t)) + \int_0^R p(r) F_r[x](t) dr$ are also shown in Fig. 4 with $g(x(t)) = -x^3(t) + 2.42x(t)$. As a contrast, the modified P-I model indeed describes the asymmetric loops depending on $g(x(t))$.

III. HYSTERESIS COMPENSATION

In this section, the direct inverse hysteresis compensation controller is designed with the developed hysteresis model. Different from the commonly used inverse compensation method reported in the literature, the proposed method avoids the complex and difficult mathematical procedure for developing an inversion of the hysteresis model. In the

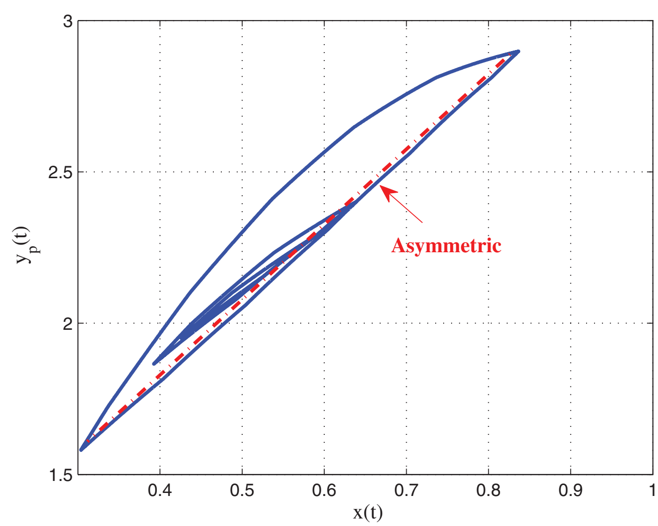

FIG. 4. Hysteresis loops generated by the modified P-I model (4).

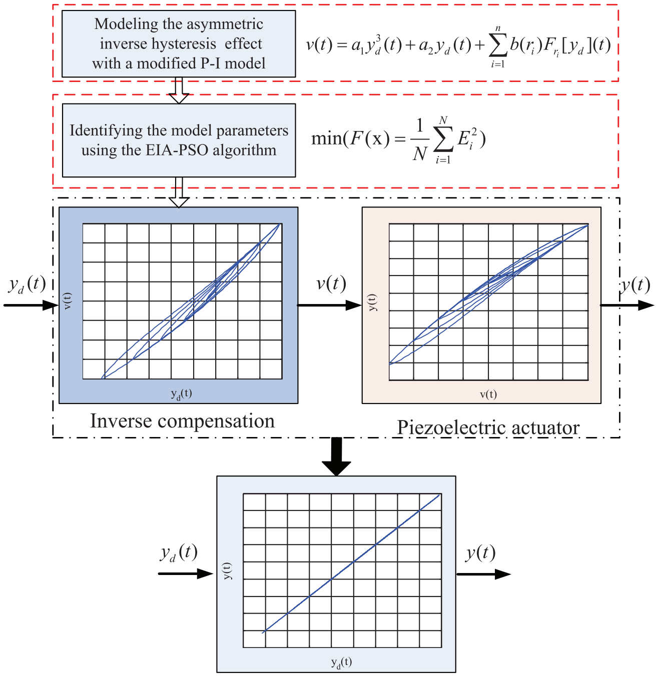

FIG. 5. Flow chart of inverse hysteresis compensation.

following development, the modified P-I model (4) is first applied to characterize the inverse hysteresis loops. According to the experimental data, the effective informed adaptive particle swarm optimization (EIA-PSO) algorithm[30] is utilized to obtained the parameters of the modified P-I model. A feedforward controller is then designed with the identified model parameters to linearize the hysteresis nonlinearity, which forces the actual trajectory $y(t)$ to follow the desired trajectory $y_d(t)$. Figure 5 shows the flow chart of the inverse hysteresis compensation method. In addition, real-time hysteresis compensation also requires the availability of sufficiently fast algorithms for implementation. The sampling frequency is set to 20 KHz in the real-time feedforward controller.

A. Feedforward controller

To calculate the compensation signal in a digital signal processor, a discrete form of the modified P-I model (4) is used for real-time inverse compensation as follows:

$$v(t) = a_1 y_d^3(t) + a_2 y_d(t) + \sum_{i=1}^{n} b(r_i) F_{r_i}[y_d](t), \tag{5}$$

where n is the number of the adopted play operators for modeling, and $b(r_i)$ is the weighted constant for the threshold r_i. Generally, the larger n is selected, it is more precision to describe the inverse hysteresis loops. On the other hand, more efforts should be made in the real-time calculation of compensation signal. In this work, ten play operators (i.e., $n = 10$) are chosen for identification and compensation with fixed threshold values r_i, which are determined as

$$r_i = \frac{i}{n}||y_d(t)||_\infty, \ i = 0, 1, 2, \ldots, n-1 \tag{6}$$

with $||y_d(t)||_\infty = 1$ in the normalized case.

Remark: It should be noted that in this work the modified P-I model is directly adopted to characterize the inverse hysteresis effect. The difference between the inverse hysteresis and the real hysteresis in the piezoelectric actuator is the orientation of the hysteresis loops, which is distinguished by the sign of the weighted function. Therefore, the play operator F_r in (5) is the same as the one in (3) and (4).

B. Parameters identification

In order to implement the real-time feedforward controller, the main challenge lies on weighted parameters identification to establish the modified P-I model (5) for matching the experimental inverse hysteresis loops. Due to the nonlinearity characteristics, it is difficult to effectively identify the parameters.[32] As an illustration of this work, the EIA-PSO algorithm[30] is introduced for simultaneous identification of all the weighted parameters and coefficients of the polynomial input function with the fixed threshold values r_i in (6). Certainly, other optimization algorithms, for instance, the constrained quadratic optimization algorithm and unconstrained nonlinear optimization algorithm, can also be used. Without loss of generality, in what follows we use the EIA-PSO algorithm to validate the proposed model and develop the corresponding controller.

Generally, the selection of the objective function has important influence on the parameter identification result. In this work, the objective function is chosen as

$$F(\mathbf{x}) = \frac{1}{N}\sum_{i=1}^{N} E_i^2 \tag{7}$$

with

$$E_i = v_i - v_i^a, \tag{8}$$

where $\mathbf{x} = [a_1, a_2, b_1, b_2, \ldots, b_{10}]$ is a set of identified parameters of the modified P-I model, which is unknown for the actual system; N denotes the number of experimental data for identification; E_i is the error between the model simulation data v_i and real experimental data v_i^a at the ith sampling time. The optimization objective herein is to find the effective parameter values $\mathbf{x}$ that can minimize the objective function $F(\mathbf{x})$ in (7) with respect to the experimental data. In this work, the identification algorithm is off-line carried out in the MATLAB environment. The reader may refer to Ref. 30 for detailed description of the EIA-PSO algorithm. Table I lists the identified model parameters. Figure 6 shows the comparison of the model simulation output and experimental data for validation, where the estimated errors are less than 1% of the total range as shown in Fig. 7. It is worth mentioning that although the parameters is obtained by using the simple identification signals, the following experimental results shall demonstrate the excellent effectiveness of the inverse hysteresis compensation controller with these identified parameters under various typical kinds of referenced trajectories.

TABLE I. Identified parameters of the modified P-I model.

Number	r_i	b_i	a_i
1	0	−0.00002	0.1608
2	0.1	−0.26603	1.2588
3	0.2	−0.10684	
4	0.3	−0.01221	
5	0.4	−0.08412	
6	0.5	−0.00238	
7	0.6	−0.00328	
8	0.7	−0.01115	
9	0.8	−0.03417	
10	0.9	−0.47999	

IV. EXPERIMENTAL VALIDATION

A. Experimental setup

As shown in Fig. 8, an experimental platform is built in this work for inverse hysteresis compensation of the piezoelectric actuator. A preloaded piezoelectric stack actuator (PPSA) PSt 150/7/100 VS12 from Piezomechanik in Germany is adopted to drive the one-dimensional flexure hinge guiding nanopositioning stage with the nominal 75 μm displacement. The PPSA is driven by a high-voltage amplifier with a fixed gain of 15, which thus provides excitation voltage for the PPSA in the 0–150 V range. A high-resolution strain gauge position sensor is integrated in the PPSA to measure the real-time position for parameters identification. Then, the real-time position is captured by the position servo-control module, which transfers the actual displacement to analogue voltage in the range of 0–10 V. To control of the piezoelectric actuator, the dSPACE-DS1103 rapid prototyping controller board equipped with 16-bit DACs and 16-bit ADCs is used to implement the inverse hysteresis compensation algorithm. For the purpose of fast inverse compensation, the sampling frequency of the dSPACE control system is set to 20 kHz. In the controller design using the dSPACE system, the control voltage $v(t)$ is normalized to 0–1 V with respect to the 0–10 V range, while the real-time displacement signal $y(t)$ is normalized with the maximum displacement of 75 μm.

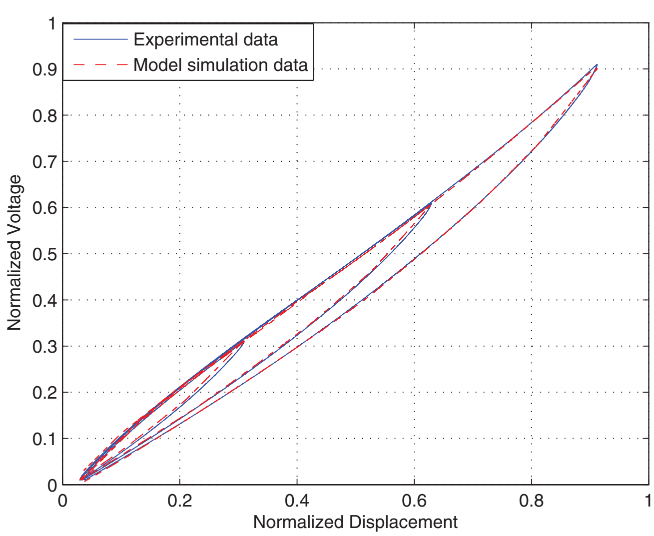

FIG. 6. Comparison of the model simulation output and experimental data.

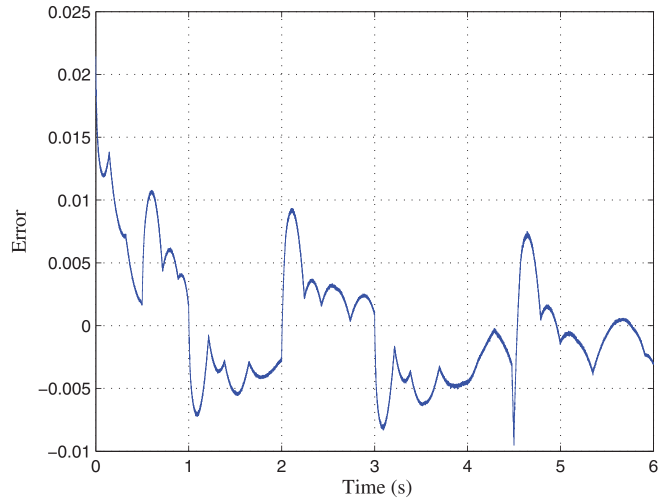

FIG. 7. Estimated error.

B. Experimental tests

To verify the effectiveness of the proposed inverse compensation method with the modified P-I model, several experimental tests are conducted with various typical referenced trajectories.

1. Triangular trajectory

The triangular trajectory is a typical waveform for scanning applications of piezoelectric actuators especially in the SPMs or AFMs.[1–3] In this work, the first test is done to follow the triangular referenced trajectory. Figure 9 shows the tracking performance of the inverse compensation controller

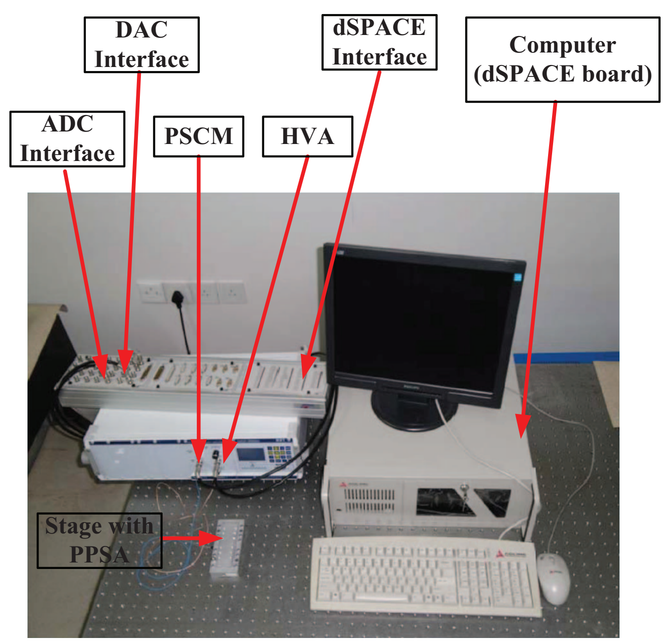

FIG. 8. The experimental platform.

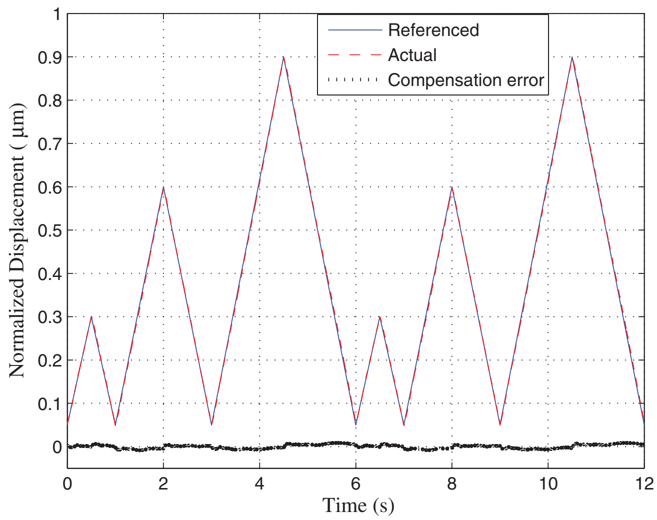

FIG. 9. Tracking performance of the inverse compensation controller with a triangular trajectory (blue solid-referenced trajectory; red dashed-actual trajectory with the inverse compensation; black dottted-tracking error).

with a triangular trajectory. From the experimental results, the maximum tracking error is less than 1% with the proposed feedforward controller. However, the hysteresis caused error is about 12% if the inverse compensation controller is not implemented. Therefore, the hysteresis caused error is reduced by about 90% using the proposed hysteresis compensation approach compared with no inverse hysteresis compensation. Figure 10 shows the control voltage generated by the feedforward controller, where it is not the perfect triangular signal and thus can compensate for the hysteresis nonlinearity. To illustrate the hysteresis compensation more clearly, Fig. 11 summarizes three input-output relationships in terms of desired displacement vs control voltage, control voltage vs actual displacement, and desired displacement vs actual displacement. It can be seen that feedforward controller indeed generates the inverse hysteresis loops (indicated by the red dashed line in Fig. 11) compared with the real

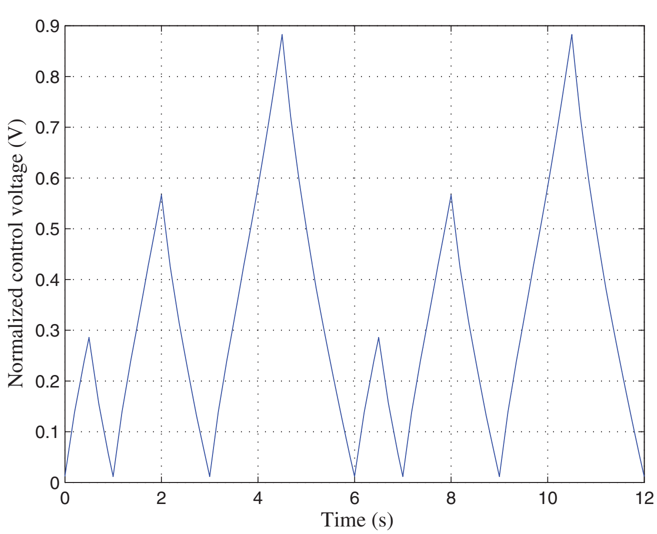

FIG. 10. Control voltage generated by the feedforward controller with a triangular trajectory.

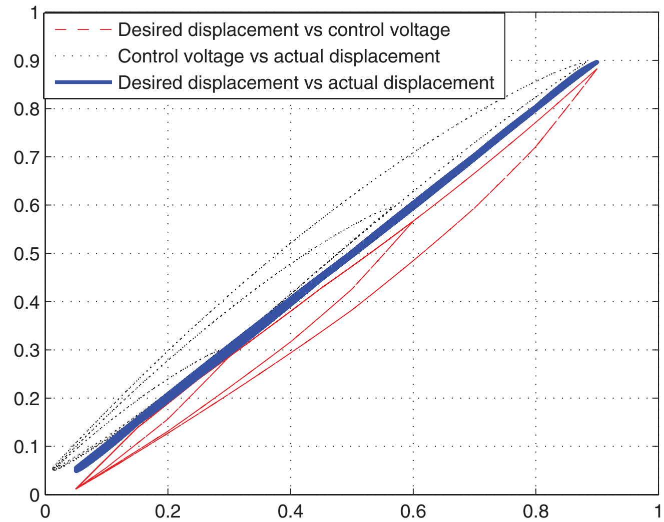

FIG. 11. Three kinds of input-output relationships with a triangular trajectory (red dashed-desired displacement vs control voltage; black dotted-control voltage vs actual displacement; blue solid-desired displacement vs actual displacement).

hysteresis nonlinearity in the piezoelectric actuator (indicated by the black dotted line in Fig. 11), and thus achieves the approximate linear relationship between the desired displacement and the actual displacement indicated by the blue solid line in Fig. 11, which demonstrates the effectiveness of the inverse hysteresis compensation method.

2. Step-like trajectory

As the step-like trajectory is generally used to validate the inverse hysteresis compensation controllers in the literature,[21,31] we have also used this type of trajectory as our reference for validation. The experimental results are shown in Figs. 12 and 13. By introducing the inverse compensation controller, the generated control voltage as shown in Fig. 13

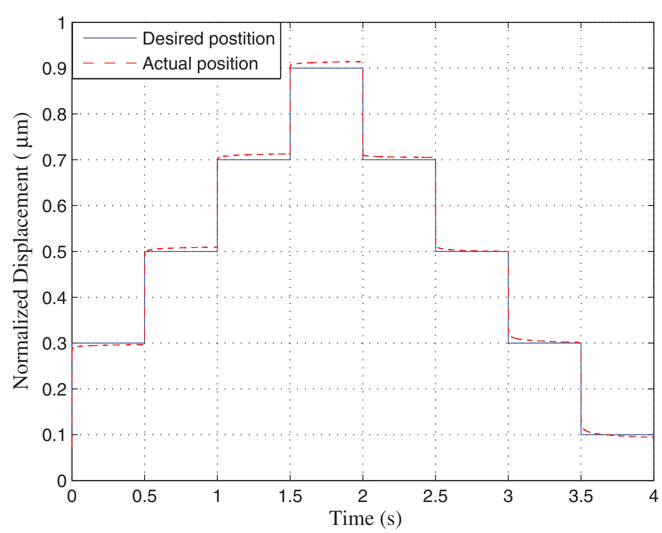

FIG. 12. Tracking performance of the inverse compensation controller with a step-like trajectory (blue solid-referenced trajectory; red dashed-actual trajectory with the inverse compensation.

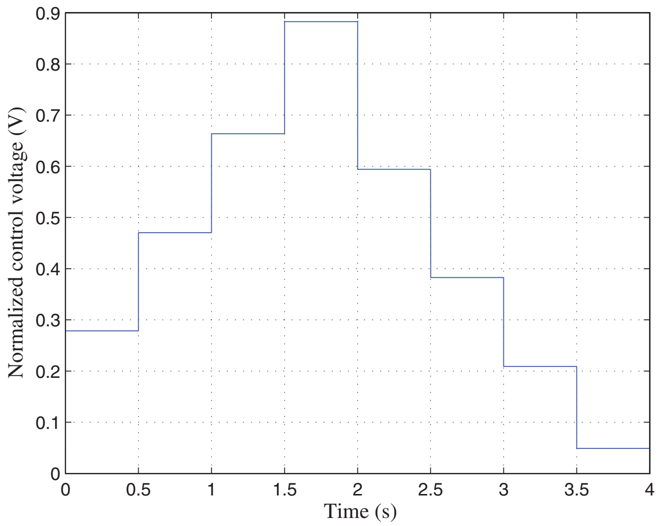

FIG. 13. Control voltage generated by the feedforward controller with a step-like trajectory.

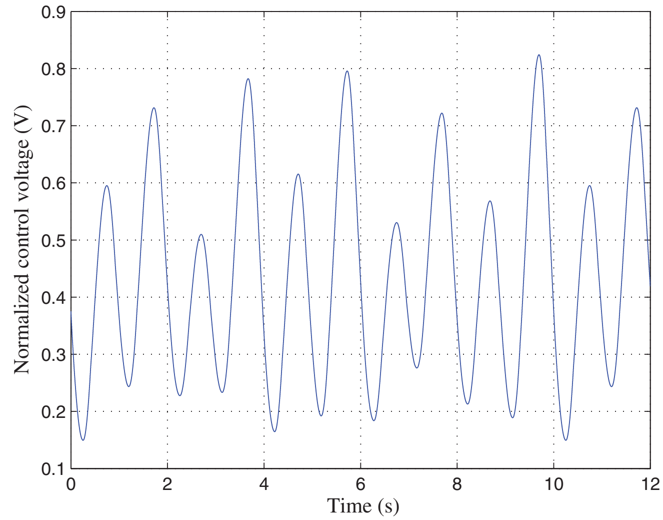

FIG. 15. Control voltage generated by the feedforward controller with a complex trajectory.

is asymmetric for the symmetric step-like referenced trajectory, and therefore cancels the real hysteresis nonlinearity in the piezoelectric actuator. From Fig. 12, it can be observed that the hysteresis nonlinearity is greatly reduced. It should be noted that the proposed method focuses on the hysteresis compensation, and the related creep compensation is not considered in this paper. In fact, the creep can be characterized by a definite mathematic model. It is more convenient to be compensated by the feedforward control method as be recommended in Refs. 12, 33, and 34, which is not discussed in this work.

3. Complex trajectory

To further elucidate the advantages of the proposed inverse hysteresis compensation method, tracking experiments with a complex non-periodic trajectory are conducted. The experimental results are shown in Figs. 14–16. Figure 14 shows the actual trajectory and the tracking errors for the referenced trajectory. Figure 15 shows the input control signal $v(t)$. Figure 16 illustrates how the feedforward controller linearizes the hysteresis nonlinearity, where both the inverse major-loop and minor-loop hysteresis loops with asymmetric characteristics are produced by the feedforward controller to cancel the corresponding real hysteresis effect.

As evident from the results presented in Figs. 9–16, the proposed inverse controller with the modified P-I model effectively overcomes the effects of the hysteresis and demonstrates excellent tracking performance. Furthermore, the proposed method is simpler and easier to be implemented in real time.

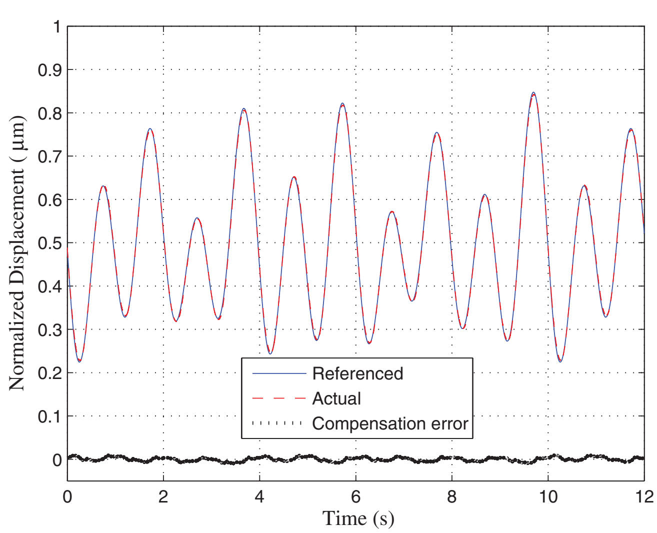

FIG. 14. Tracking performance of the inverse compensation controller with a complex trajectory (blue solid-referenced trajectory; red dashed-actual trajectory with the inverse compensation; black dotted-tracking error).

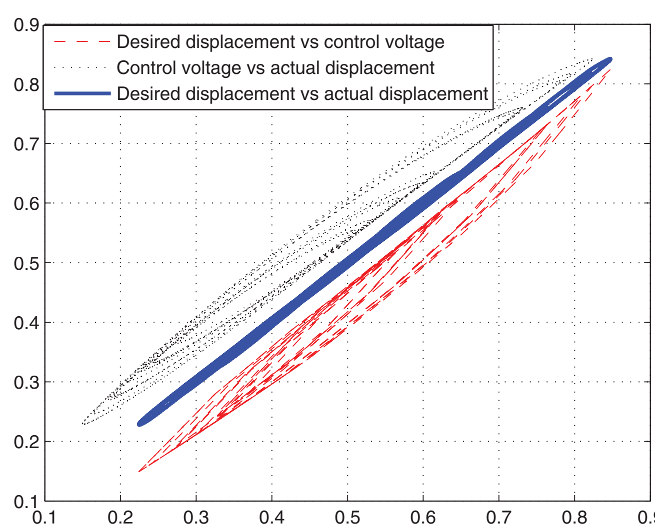

FIG. 16. Three kinds of input-output relationships with a complex trajectory (red dashed-desired displacement vs control voltage; black dotted-control voltage vs actual displacement; blue solid-desired displacement vs actual displacement).

V. CONCLUSION

In this paper, a real-time inverse hysteresis compensation method with a modified P-I model is presented, and experiments on a piezoelectric actuated platform have also been conducted to demonstrate its feasibility and effectiveness. Several distinct features of this paper are summarized as follows:

(i) A modified P-I model is first developed to describe the asymmetric hysteresis characteristics. On the basis of the classical P-I model, the improved P-I model is defined in terms of weighted one-side play operators and a polynomial input function. With this model, the hysteresis shapes can be determined by not only the weighted play operators but also the input function. It is the modified input function that makes the developed model accommodate a more general class of hysteresis shapes. Hence, the developed model is feasible to characterize the asymmetric inverse hysteresis effect of the piezoelectric actuator.

(ii) Rather than modeling the hysteresis effect, a real-time feedforwad controller is designed through directly modeling the inverse hysteresis effect of the piezoelectric actuator with the modified P-I model. It avoids the complex and difficult mathematical procedure for developing an inversion of the hysteresis model commonly used in the literature.

(iii) Finally, an experimental platform is established. An EIA-PSO algorithm is adopted to identify the model parameters for implementation of the real-time feedforward controller. The experimental results with various typical trajectories demonstrate that the tracking errors caused by the hysteresis nonlinearity are reduced by about one order of magnitude with the proposed method.

In the future, the creep and vibration of piezoelectric actuators will be compensated to further improve the tracking performance of the piezoelectric actuated systems.

ACKNOWLEDGMENTS

This work was in part supported by the National Natural Science Foundation of China under Grant No. 91023047, the Science and Technology Commission of Shanghai Municipality under Grant No. 11520701500, and the “Shu Guang” Project supported by Shanghai Municipal Education Commission under Grant No. 10SG17.

[1] S. M. Salapaka and M. V. Salapaka, IEEE Control Syst. Mag. **28**, 65–83 (2008).
[2] Y. Li and J. Bechhoefer, Rev. Sci. Instrum. **78**, 013702 (2007).
[3] G. M. Clayton, S. Tien, K. K. Leang, Q. Zou, and S. Devasia, J. Dyn. Syst., Meas., Control **131**, 061101 (2009).
[4] D. A. Bristow, J. Dong, A. G. Alleyne, P. Ferreira, and S. Salapaka, Rev. Sci. Instrum. **79**, 103704 (2008).
[5] L. J. Lai, G. Y. Gu, and L. M. Zhu, Rev. Sci. Instrum. **83**, 045105 (2012).
[6] G. Tao and P. V. Kokotovic, IEEE Trans. Autom. Control **40**, 200–212 (1995).
[7] C. Y. Su, Y. Feng, H. Hong, and X. Chen, Int. J. Control **82**, 1786–1793 (2009).
[8] A. J. Fleming and S. O. R. Moheimani, IEEE Trans. Control Syst. Technol. **14**, 33–44 (2006).
[9] A. J. Fleming and K. K. Leang, Ultramicroscopy **108**, 1551–1557 (2008).
[10] S. Devasia, E. Eleftheriou, and S. O. R. Moheimani, IEEE Trans. Control Syst. Technol. **15**, 802–823 (2007).
[11] K. K. Leang and S. Devasia, in *Proceedings of the 2nd IFAC Conference on Mechatronic Systems* (IFAC, 2002), pp. 283–289.
[12] M. Rakotondrabe, IEEE. Trans. Autom. Sci. Eng. **8**, 428–431 (2010).
[13] C. Y. Su, Q. Q. Wang, X. K. Chen, and S. Rakheja, IEEE Trans. Autom. Control **50**, 2069–2074 (2005).
[14] G. Y. Gu and L. M. Zhu, Sens. Actuators, A **165**, 202–209 (2011).
[15] C. Visone, J. Phys.: Conf. Ser. **138**, 012028 (2008).
[16] P. Ge and M. Jouaneh, IEEE Trans. Control Syst. Technol. **4**, 209–216 (1996).
[17] G. Song, J. Q. Zhao, X. Q. Zhou, and J. A. de Abreu-Garcia, IEEE/ASME Trans. Mechatron. **10**, 198–209 (2005).
[18] H. Hu and R. B. Mrad, Mech. Syst. Signal Process. **18**, 169–185 (2004).
[19] X. Tan and J. S. Baras, IEEE Trans. Autom. Control **50**, 827–839 (2005).
[20] M. Brokate and J. Sprekels, *Hysteresis and Phase Transaitions* (Springer, 1996).
[21] P. Krejci and K. Kuhnen, IEE Proc.: Control Theory Appl. **148**, 185–192 (2001).
[22] K. Kuhnen, Eur. J. Control **9**, 407–418 (2003).
[23] M. Al Janaideh, S. Rakheja, and C. Y. Su, IEEE/ASME Trans. Mechatron. **16**, 734–744 (2011).
[24] J. M. Cruz-Hernandez and V. Hayward, IEEE Trans. Control Syst. Technol. **9**, 17–26 (2001).
[25] C. H. Ru and L. N. Sun, Rev. Sci. Instrum. **76**, 095111 (2005).
[26] G. Y. Gu and L. M. Zhu, Rev. Sci. Instrum. **81**, 085104 (2010).
[27] Q. S. Xu and P. K. Wong, Mechatronics **21**, 1239–1251 (2011).
[28] M. Rakotondrabe, C. Clevy, and P. Lutz, IEEE. Trans. Autom. Sci. Eng. **7**, 440–450 (2010).
[29] D. Croft, G. Shed, and S. Devasia, ASME J. Dyn. Syst., Meas., Control **123**, 35–43 (2001).
[30] Q. Li, W. Chen, Y. Wang, S. Liu, and J. Jia, IEEE Trans. Ind. Electron. **58**, 2410–2419 (2011).
[31] H. Janocha and K. Kuhnen, Sens. Actuators, A **79**, 83–89 (2000).
[32] Y. Li and Q. Xu, IEEE Trans. Control Syst. Technol. **18**, 798–810 (2010).
[33] H. Jung, J. Y. Shim, and D. Gweon, Rev. Sci. Instrum. **71**, 3436–3440 (2000).
[34] C. H. Ru and L. N. Sun, Sens. Actuators, A **122**, 124–130 (2005).